

# The Hierarchical Origin of Galaxy Morphologies

Matthias Steinmetz<sup>1</sup>

*Steward Observatory, 933 N Cherry Ave, Tucson, AZ 85721, USA*

Julio F. Navarro<sup>2</sup>

*Department of Physics and Astronomy, University of Victoria, Victoria, BC,  
V8P 1A1, Canada*

---

## Abstract

We report first results from a series of N-body/gasdynamical simulations designed to study the origin of galaxy morphologies in a cold dark matter-dominated universe. The simulations include star formation and feedback and have numerical resolution sufficiently high to allow for a direct investigation of the morphology of simulated galaxies. We find, in agreement with previous theoretical work, that the presence of the main morphological components of galaxies—disks, spheroids, bars—is regulated by the mode of gas accretion and intimately linked to discrete accretion events. In the case we present, disks arise from the smooth deposition of cooled gas at the center of dark halos, spheroids result from the stirring of preexisting disks during mergers, and bars are triggered by tides generated by satellites. This demonstrates that morphology is a transient phenomenon within the lifetime of a galaxy and that the Hubble sequence reflects the varied accretion histories of galaxies in hierarchical formation scenarios. In particular, we demonstrate directly that disk/bulge systems can be built and rebuilt by the smooth accretion of gas onto the remnant of a major merger and that the present-day remnants of late dissipative mergers between disks are spheroidal stellar systems with structure resembling that of field ellipticals. The perplexing variety of galaxy morphologies is thus highly suggestive of—and may actually even demand—a universe where structures have evolved hierarchically.

*Key words:* cosmology, dark matter, galaxies: formation, galaxies: structure

---

<sup>1</sup> Alfred P. Sloan Fellow & Packard Fellow. E-mail: msteinmetz@as.arizona.edu

<sup>2</sup> CIAR Scholar & Alfred P. Sloan Fellow. E-mail: jfn@uvic.ca

## 1 Introduction

The bewildering variety of galaxy morphologies has long marveled and challenged astronomers (Hubble 1926). Disks, bulges, halos, bars, tails; accounting for these basic features of galaxy taxonomy has elicited much controversy in the past, but is now widely ascribed to the particular history of mergers and accretion events that galaxies experience during their assembly in a hierarchical universe (Kauffmann et al. 1993, Baugh et al. 1998). In such scenarios, one example of which is the popular cold dark matter (CDM) cosmogony, disks are envisioned to form as the result of gas accreted smoothly from the intergalactic medium (see, e.g., Katz & Gunn 1991, Navarro & White 1994, Steinmetz & Müller 1994), whereas spheroids are the remnants of major merger events where disks are thrown together and mixed violently on a short timescale (Toomre 1977, Barnes & Hernquist 1992). Galaxy morphology thus evolves continuously throughout a galaxy’s lifetime, and is determined by a delicate balance between the mode of gas accretion and the detailed merger history of an individual galaxy. Here we present a cosmological gasdynamical simulation which confirms that a single galaxy in the CDM cosmogony may run through the whole Hubble sequence during its lifetime, validating previous theoretical expectation and illustrating the inextricable link between morphology and the hierarchical mode of galaxy formation.

## 2 The Simulation

The continual metamorphosis of galaxy morphologies in hierarchically clustering universes is well illustrated by the evolutionary sequence shown in Figures 1 to 5. These figures show, at various times, the ‘luminous’ (baryonic) component of a massive dark halo ( $\sim 2.5 \times 10^{12} M_{\odot}$  at  $z=0$ ) formed in the  $\Lambda$ CDM cosmogony (Bahcall et al. 1999).  $\Lambda$ CDM assumes a low-density universe ( $\Omega_0 = 0.3$ ), currently dominated by a cosmological constant ( $\Omega_{\Lambda} = 0.7$ ), with a baryonic density parameter  $\Omega_b = 0.019 h^{-2}$ , and a Hubble parameter  $h = H_0/(100 \text{ km s}^{-1} \text{ Mpc}^{-1}) = 0.65$ . The  $\Lambda$ CDM power spectrum is normalized so that the present-day rms mass fluctuations on spheres of radius  $8 h^{-1} \text{ Mpc}$  is  $\sigma_8 = 0.9$ .

The evolution of this system is characterized by episodes of smooth accretion punctuated by two major merger events, one at  $z \sim 3.3$  and the second at  $z \sim 0.6$ . The simulations are performed with GRAPESPH (Steinmetz 1996), a cosmological hydrodynamics code that includes the effects of gravity, gas dynamics, and radiative cooling and heating processes. Star formation is included via a phenomenological recipe that converts unstable gas regions into stars at rates chosen to match observational constraints (Steinmetz & Navarro 1999). The

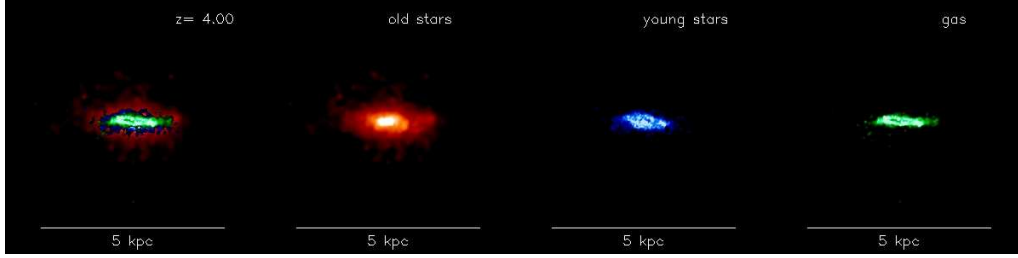


Fig. 1. The most massive progenitor at  $z=4$  shown edge-on. Gas particles are shown in green, ‘young’ (i.e. less than 200 Myr old) stars in blue and older stars in red. Horizontal bars in each panel are 5 (physical) kpc long.

simulation concentrates computational resources on the surroundings of a single dark halo identified at  $z=0$ , but it includes nonetheless the full tidal field of a large, representative volume of the  $\Lambda$ CDM cosmogony (see, e.g., Navarro & White 1994). The particle mass in the simulation is  $1.27 \times 10^7 M_\odot$  for the gas component and  $5.76 \times 10^7 M_\odot$  for the dark matter component, respectively. The Plummer gravitational softening is fixed at 0.5 (physical) kpc.

### 3 Disks and Bulges

As early as  $z=4$ , the most massive progenitor of the galaxy has already assembled  $\sim 3 \times 10^{10} M_\odot$  of gas and stars in a disk-like configuration, as shown in Figure 1. The disk is rather small, about 3 (physical) kpc in diameter, and rotates at approximately  $180 \text{ km s}^{-1}$ . In agreement with the main premise of the hierarchical scenario, the disk is the outcome of smooth accretion of gas and of its progressive transformation into stars over the lifetime of the system. Star formation begins in earnest at  $z \sim 10$  and proceeds at an average rate of  $\sim 30 M_\odot \text{ yr}^{-1}$ , albeit spread over a number of subsystems arranged along a filamentary structure. The largest of the progenitor subsystems is illustrated in Figure 1. Stars younger than 200 Myr are shown in blue, older stars in red. The “pure disk” phase in the evolution of this galaxy comes to an end rather abruptly at  $z \sim 3.3$ , when the galaxy merges with a similarly-sized companion. The merger stirs the stars from the disk components and assembles them into a single spheroidal component—the progenitor of a bulge (see the  $z=3.15$  panel in Figure 2). The merger is also accompanied by a burst of star formation that largely depletes the gas content of the merging disks, transforming  $1.6 \times 10^{10} M_\odot$  of gas into stars in just 300 Myr.

Just before the burst, the apparent brightness of the galaxy is about 26.5 mag in the  $r$ -band (assuming 1.5 mag of dust dimming), about 1 mag fainter than the current limiting magnitude of the spectroscopically-confirmed ‘Lyman-break’ population (Steidel et al. 1996). During the burst at  $z = 3.3$ , however, its maximum brightness reaches 25  $r$ -mag, compatible with that in current

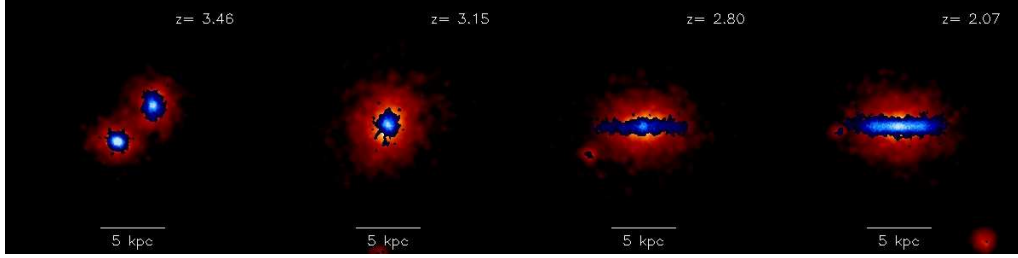


Fig. 2. The formation of a bulge and the rebirth of a disk. The sequence shows the formation of a bulge by the merger of two almost equal mass ‘pure disk’ systems at  $z \sim 3$ . After  $z=3$  smooth accretion of gas regenerates the disk component around the bulge. Blue is used in each panel to denote stars formed since the preceding frame (since  $z=4.2$  for the first panel), red for older stars. Horizontal bars in each panel are 5 (physical) kpc long.

Lyman-break spectroscopic samples. This implies that at least some of the bright Lyman-break systems may be the result of merger-triggered starbursts associated with the epoch of bulge formation (Somerville et al. 2000). We note, however, that overall the brightening during the burst is modest, and that this galaxy is not a dwarf system: its stellar mass at  $z = 3.3$  is  $6.3 \times 10^{10} M_{\odot}$ , comfortably in the range of best estimates available for the Lyman-break galaxies (Papovich et al. 2001, Rudnick 2001, Shapley et al. 2001). This result, together with the short duty cycle associated with this event (about 300 Myr) and the strong clustering of bright Ly-break systems, supports early theoretical suggestions that a substantial fraction of the Lyman-break galaxies may inhabit massive halos and may be the progenitors of bright cluster ellipticals (Baugh et al. 1998, Mo, Mao & White 1999).

#### 4 The Rebirth of a Disk Galaxy.

From  $z = 3$  to  $z = 1.8$  (see Figure 2) the baryonic mass of the galaxy increases by  $\sim 50\%$  through smooth accretion of intergalactic gas not attached to massive clumps. As expected, the accreting gas radiates its energy quite efficiently and assembles into a new, distinct disk component where star formation proceeds at a rate that declines from  $20 M_{\odot} \text{ yr}^{-1}$  at  $z \sim 3$  to  $8 M_{\odot} \text{ yr}^{-1}$  at  $z=1.8$ . The disk is clearly assembled from the inside out, although there is substantial scatter in the angular momentum of the accreting gas and non negligible amounts of late-accreting, low angular momentum gas continues to fuel star formation near the center and throughout the disk. At  $z=1.8$  the simulated galaxy resembles a bright ( $M = -22$  in  $r$ ) Sa/Sb spiral (Figure 3). Over 70% of the rest-frame optical luminosity comes from a roughly exponential disk with  $\sim 1.5$  (physical) kpc scale length while the rest comes from a spheroidal component whose spatial distribution may be well approximated by an  $r^{1/4}$ -law with a  $\sim 1$  kpc effective radius. *This is to date the most direct*

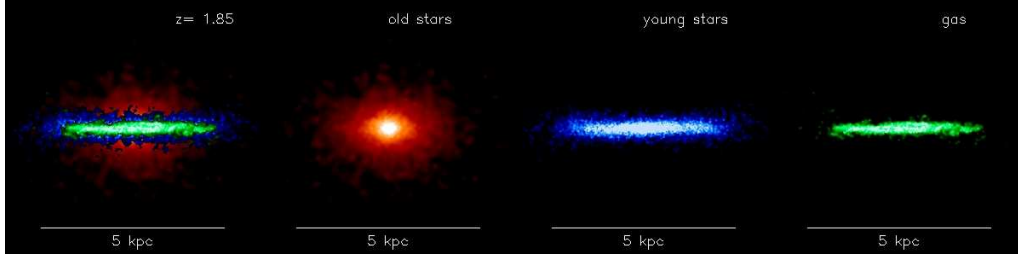


Fig. 3. The appearance of the galaxy at  $z=1.8$ , seen edge-on. Green is used for the gas, blue for ‘young’ stars (i.e. formed since  $z=3$ ), red for older stars. At this time, the morphology of the galaxy is reminiscent of early type spirals, with a dense bulge surrounded by a disk of gas and young stars. Horizontal bars in each panel are 5 (physical) kpc long.

*demonstration that rotationally supported disks of gas and young stars, as well as dynamically hot, centrally concentrated bulge-halo systems of old stars—the main luminous components of present-day disk galaxies—are natural byproducts of the hierarchical assembly of a galaxy.*

## 5 From Disk Galaxy to Barred Galaxy

Between  $z=1.8$  and  $z=0.7$  the disk undergoes a further dramatic transformation as the dominant mode of gas accretion switches from smooth buildup of intergalactic gas to the accretion of discrete satellites. The most significant of these events adds  $\sim 10\%$  of mass to the spheroidal component at  $z=1.18$ , when a close passage through the disk plane violently disrupts the satellite (few of the satellite’s stars make it into the disk), in a process highly reminiscent of the ongoing disruption of the Sagittarius dwarf by the Galaxy (Ibata et al. 1994, Helmi et al. 1999). The satellite’s main effect on the disk morphology, however, dates to its first pericentric (10 kpc) passage, at  $z=1.62$ , when the satellite’s tide forces a distinct bar pattern on the disk, clearly seen in Figure 4.

The bar pattern persists long after the disruption of the culprit satellite and its response is strongest in the gas, leading to the formation of young stars (shown in blue) that trace the bar pattern better than older disk stars (in red). The bar extends out to about 2.5 kpc and has a corotation radius of slightly less than 3 kpc, implying, in agreement with the few barred galaxies where this ratio has been measured (Debattista & Sellwood 1999), that the bar is “fast”. The baryonic component dominates the mass distribution near the center (75% of the mass within 3 kpc is in gas and stars) and the bar pattern appears stable, clearly lasting for more than 30 orbital periods. Although the process described here is likely not the only bar formation mechanism acting on real galaxies, our simulation shows nevertheless a direct link between the

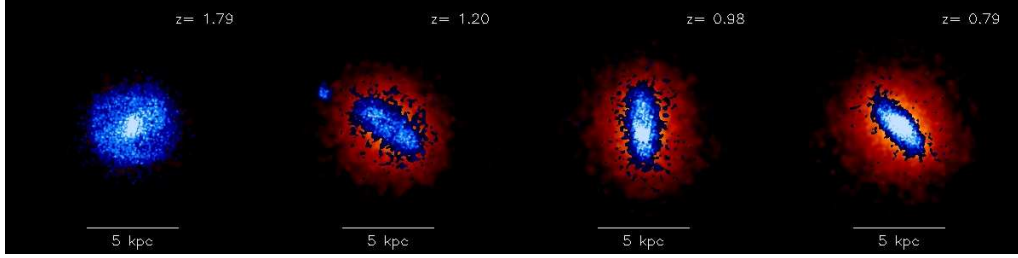


Fig. 4. The tidal triggering of bar instability by a satellite. At  $z=1.6$  the disk develops a well defined, long-lasting bar pattern as a result of tidal forcing by the satellite shown in the  $z=1.2$  panel. The satellite is finally disrupted at  $z=1.18$  after 7 pericentric passages. The bar pattern, however, survives for several Gyr, as shown in the picture. Stars less than 1.5 Gyr old are shown in blue, older stars in red. Note that the bar is most prominent in the young component. Horizontal bars in each panel are 5 (physical) kpc long.

presence of a bar pattern and the existence of satellites that may act as tidal triggers. It thus suggests that substantial insight into the accretion history of the galaxy population may be gained from studying the frequency and strength of barred patterns in spiral galaxies as a function of redshift, as highlighted in recent work (Abraham et al. 1999).

## 6 Ellipticals as the Outcome of Major Mergers

The bar pattern in the disk is still quite strong at  $z=0.7$ , when the galaxy undergoes a major merger with a companion roughly half as massive. The outcome of such major merger—a spheroidal pile of stars—has been discussed extensively in the literature since the Toomres first suggested mergers of spirals as a possible route to forming elliptical galaxies (Toomre & Toomre 1972, Toomre 1977). As illustrated in Figure 5, the final collision between the two main bodies of the colliding galaxies occurs at  $z\sim 0.6$ , and leaves behind a triaxial stellar system reminiscent of nearby field ellipticals (de Zeeuw & Franx 1991). The remaining gas within the two spirals ( $\sim 10\%$  of the total baryonic mass) is efficiently funneled to the center during the merger, where it is quickly converted into stars (Hernquist & Barnes 1991). This last episode of star formation is effectively over by  $z=0.5$ , leaving at  $z=0.27$  (rightmost panel of Figure 5) only a small ( $\sim 1$  kpc diameter) ‘core’ of metal-rich stars younger than 1.5 Gyr (in blue in Figure 5), surrounded by a large spheroid of older stars (shown in red). Exhausted its star formation fuel, stars in the galaxy evolve passively for the remaining 3.5 Gyr.

At  $z=0$  the galaxy closely resembles an elliptical both dynamically and in its stellar population. With a central (i.e. within 3 kpc) 1-d velocity dispersion of  $310 \text{ km s}^{-1}$  and a  $\sim 1.3$  kpc effective radius this  $M_r = -22$  galaxy sits close to

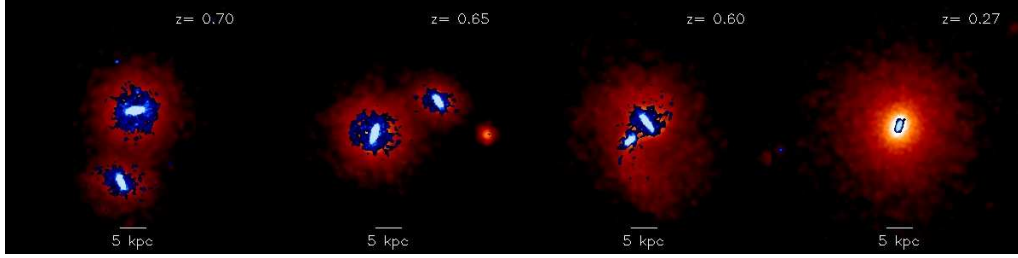


Fig. 5. A major merger and the formation of an elliptical galaxy. The disk merges with another system of about half its mass at  $z=0.7$  to form a spheroidal system of stars resembling an elliptical galaxy. All remaining gas is driven to the center of the remnant and consumed in a burst of star formation lasting 600 Myr. Stars less than 1.5 Gyr old are shown in blue, older in red. A movie illustrating the whole evolution of the galaxy can be found in the supplemental material associated with this manuscript.

the ‘Fundamental Plane’ drawn by ellipticals at  $z = 0$  (Jorgensen et al. 1996), although its radius seems significantly smaller than typical ellipticals of this luminosity. The stellar body of the galaxy is mildly triaxial, and rotates around its minor axis at a maximum speed of  $\sim 200 \text{ km s}^{-1}$ , with little indication of large misalignments between its dynamical and structural axes. Its mean color,  $B - V = 1.0$  (Vega magnitudes), is also consistent with those of bright spheroids in the local universe, and even the presence of a slightly younger ‘core’ bears a striking resemblance to the detailed structure of field ellipticals recently unveiled by Hubble Deep Field studies (Menanteau et al. 2001).

## 7 Summary

The evolutionary sequence portrayed in Figures 1 to 5 demonstrates conclusively the ever-changing nature of galaxy morphology and the intimate connection between morphology and accretion history. The perplexing variety of observed galaxy morphologies thus arises naturally in a hierarchical universe, where structures are assembled through a combination of mergers and smooth accretion. Our study confirms early theoretical work regarding the origin of all major components making up present-day galaxies. In particular, the simulation presented here shows that (i) most of the stars that make up the halo and bulge of disk galaxies may have been born in early proto-disks that were later stirred into spheroids by mergers, (ii) that disk/bulge systems may be formed by smooth accretion of gas onto the remnants of major mergers, (iii) that the population of Lyman-break galaxies may include some ongoing merger events associated with the formation of the first spheroids, and (iv) that the remnants of late dissipative disk mergers are spheroidal stellar systems with structure resembling that of field ellipticals.

These results provide clear support for the long-held view that the Hubble sequence can be understood in terms of accretion histories and that morphology is a transient phenomenon in the lifetime of a galaxy. Our study also highlights some of the potential shortcomings of hierarchical galaxy formation scenarios. For example, is the large fraction of stars observed in disks today consistent with the ‘lumpy’ accretion histories expected in CDM-like scenarios? Can one account for the observed frequency, size, and dynamical properties of ‘pure disk’ (bulge-less) galaxies? Can variations in accretion history with environment account for the morphology-density relation? These questions are critical to the success of the hierarchical model and remain challenging puzzles to be elucidated within this so far highly successful paradigm. It will take a substantive computational effort to address them through direct simulation, but one that is within reach of today’s technological capabilities. We look forward to a new era when galaxy morphology will reach beyond its wondrous aesthetic appeal and will fulfill its promise to decipher the intricate paths of galaxy formation.

## 8 Acknowledgments

This work has been supported by the National Aeronautics and Space Administration under NASA grants NAG 5-7151 and NAG 5-10827, NSF grant 9870151 and by NSERC Research Grant 203263-98. MS and JFN are supported in part by fellowships from the Alfred P. Sloan Foundation. MS is also supported by a fellowship from the David and Lucile Packard Foundation.

## References

- Abraham, R.G., Merrifield, M.R., Ellis, R.S., Tanvir, N.R., & Brinchmann, J. 1999, MNRAS, 308, 569
- Barnes, J.E. & Hernquist, L.E. 1992, ARA&A, 30, 705
- Bahcall, N.A., Ostriker, J.P., Perlmutter, S., & Steinhardt, P.J. 1999, Science, 284, 1481
- Baugh, C.M., Cole, S., Frenk, C.S., & Lacey, C.G. 1998, ApJ, 498, 504
- Debattista, V.P., & Sellwood, J. 1999, ApJ, 493, L5
- de Zeeuw, T., & Franx, M. 1991, ARA&A, 29, 239
- Helmi, A., White, S.D.M., de Zeeuw, P.T., & Zhao, H. 1999, Nature, 402, 53
- Hernquist, L.E., & Barnes, J.E. 1991, Nature, 354, 210



- Hubble, E.P. 1926, ApJ, 64, 321
- Ibata, R.A., Gilmore, G., & Irwin, M.J. 1994, Nature, 370, 194
- Jorgensen, I., Franx, M., & Kjaergaard, P. 1996, MNRAS, 280, 167
- Katz, N., & Gunn, J.E. 1991, ApJ, 377, 365
- Kauffmann, G., White, S.D.M., & Guiderdoni, B. 1993, MNRAS, 264, 201
- Menanteau, P., Abraham, R.G., & Ellis, R. 2001, MNRAS, 322, 1
- Mo, H.-J., Mao, S. & White S.D.M. 1999, MNRAS, 304, 175
- Navarro, J.F., & White, S.D.M. 1994, MNRAS, 267, 401
- Papovich C., Dickinson, M., Ferguson, H.C. 2001, ApJ, 559, 620
- Rudnick, G., 2001, PhD thesis, University of Arizona
- Shapley, A.E., Steidel, C.C., Adelberger, K.L., Dickinson, M., Giavalisco, M., Pettini, M. 2001, ApJ, 562, 95
- Somerville, R.S., Primack, J.R., & Faber, S.M. 2001, MNRAS, 320, 504
- Steidel, C.S., Giavalisco, M., Pettini, M., Dickinson, M., & Adelberger, K.L. 1996, ApJ, 462, 17
- Steinmetz, M. 1996, MNRAS, 278, 1005
- Steinmetz, M., & Müller, E. 1994, A&A, 281, L97
- Steinmetz, M., & Navarro, J.F. 1999, ApJ, 513, 555
- Toomre, A. 1977, IAUS, 58, 347
- Toomre, A., & Toomre, J. 1972, ApJ, 178, 623